Inorganic Chemistry

Article

pubs.acs.org/IC

An Inorganic Chromophore Based on a Molecular Oxide Supported Metal Carbonyl Cluster: $[P_2W_{17}O_{61}\{Re(CO)_3\}_3\{ORb(H_2O)\}(\mu_3\text{-}OH)]^{9-}$

Chongchao Zhao, William Rodríguez-Córdoba,† Alexey L. Kaledin, Ye Yang, Yurii V. Geletii, Tianquan Lian,* Djamaladdin G. Musaev,* and Craig L. Hill*

Department of Chemistry and Cherry L. Emerson Center for Scientific Computation, Emory University, Atlanta, Georgia 30322, United States

Supporting Information

ABSTRACT: A polyoxometalate-supported trirhenium carbonyl cluster, mimicking metal oxide supported interfacial dyadic structures, has been synthesized and characterized. Multiple techniques, including computational and transient absorption spectroscopy, have been applied to characterize the charge-transfer dynamics occurring at the interfaces of this "double cluster". The stepwise kinetics of charge separation and recombination has been thoroughly investigated.

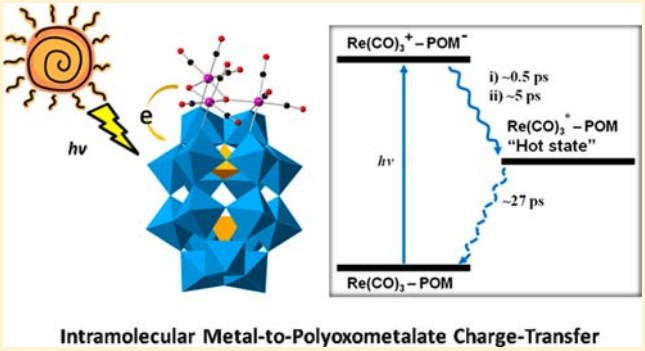

Intramolecular Metal-to-Polyoxometalate Charge-Transfer

INTRODUCTION

Dyadic systems comprising a metal-to-ligand charge-transfer (MLCT) chromophore $[Ru(bpy)_3]^{2+}$ (and its derivatives) and semiconductor metal oxide acceptor, most frequently TiO_2, form the basis of dye-sensitized solar cell (DSSC) technology.[1] Since the original Grätzel $[Ru(bpy)_3]^{2+}$-TiO_2 dyadic structures, there has been and continue to be major efforts to study and optimize the photodynamic, stability, and optical properties of these promising systems. More recently, these systems have been coupled with water oxidation catalysts to function as triadic photoanodes for water oxidation.[2] However, these systems show limited stability under water oxidizing conditions, primarily because the organic ligands (usually *bpy*) get oxidized. As a consequence, there have been major recent efforts to prepare metal-to-metal charge-transfer (MMCT) chromphores containing no organic ligands, including extensive work on bimetallic assemblies supported on mesoporous silica reported by Frei and co-workers.[3] However, all the above-mentioned dyadic configurations are heterogeneous in nature making it very difficult to acquire a precise atomistic level understanding of their physicochemical properties. In this paper we report a homogeneous dyadic structure in the form of a multimetal electron donor unit attached to the outside of a polyoxometalate (POM) electron acceptor unit, $[P_2W_{17}O_{61}\{Re(CO)_3\}_3\{ORb(H_2O)\}(\mu_3\text{-}OH)]^{9-}$ (**1**). Like TiO_2 and most other semiconductor metal oxides of interest in solar energy conversion,[4] the POM ligand in **1** is readily reduced at low energy (modest reduction potentials in solution of −0.4 to −0.8 V versus NHE).[5] Compound **1** is a new kind of chromophore with little or no oxidizable organic structure for possible use in solar fuel production assemblies. This investigation includes a comprehensive characterization of the geometrical and electronic structure of **1** using several spectroscopic methods, X-ray crystallography, time-resolved methods, and computational studies.

RESULTS AND DISCUSSION

Compound **1** is prepared by the reaction of a POM precursor, $[P_4W_{35}O_{124}\{Re(CO)_3\}_2]^{16-}$,[6] and $[Re(CO)_3]^+$ complexes in a slightly acidic (pH = 5−6) aqueous solution (see Supporting Information). The crystal structure of **1** (Figure 1a) reveals an "out-of-pocket" motif[7] with a trirhenium carbonyl "cap" grafted on the defect site of $[\alpha_2\text{-}P_2W_{17}O_{61}]^{10-}$ (the "support"). The Re−C bond lengths range from 1.87 to 1.92 Å, while the C−O bonds range from 1.15 to 1.21 Å. It should be noted that POM-supported metal carbonyl complexes constitute molecular models for metal-oxide-supported metal−carbonyl catalysts.[8] Several have been prepared previously but all these complexes contain only a mononuclear $\{M(CO)_x\}^+$ unit (or separated mononuclear units).[6,9] Compound **1** is the first with an oxo-centered multimetal electron donor substructure. Interestingly, the three Re(I) centers reside in different coordination environments (Figure 1b). Re1 and Re2 are similar and bonded by O1 and O2 forming one Re−O−W bond to $[\alpha_2\text{-}P_2W_{17}O_{61}]^{10-}$. In contrast, Re3 is bonded to O1 and forms two Re−O−W bonds to the POM moiety. An aqua alkali metal moiety $[Rb(H_2O)]^+$ (bonded to disordered O11w and O12w with an occupancy of 0.5 for each) is also strongly (2.80 Å bond distance) bonded to O2. The Rb^+ cation further coordinates to

Received: July 21, 2013
Published: November 15, 2013

   dx.doi.org/10.1021/ic4018823 | *Inorg. Chem.* 2013, 52, 13490−13495

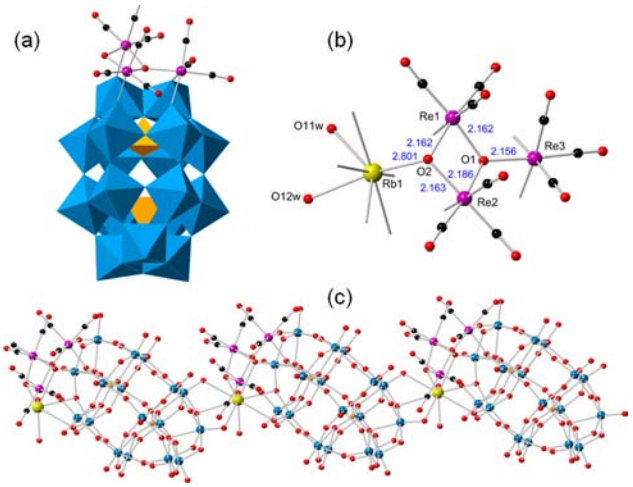

Figure 1. (a) X-ray structure of **1** in combined ball-and-stick and polyhedral representations ($[Rb(H_2O)]^+$ is omitted for clarity). Re, purple; O, red; C, black; WO_6 octahedra: blue; PO_4 tetrahedra: gold. (b) Top view of the trirhenium "cap" (including the $[Rb(H_2O)^+]$ unit) with representative bond distances (Å). The bridging oxygens to the POM are omitted. (c) Ball-and-stick representation of the quasi-1D chain of **1** along the *b*-axis.

the bridging/terminal oxo ligands in the adjacent POMs with distances ranging from 2.84 to 3.14 Å, defining a quasi-1D chain (Figure 1c).

The central atom, O1, can be assigned as hydroxide, that is, μ_3-OH, based on several arguments: (1) the "cap" $[\{Re(CO)_3\}_3\{ORb(H_2O)\}(\mu_3\text{-}OH)]^+$ is positively charged which makes it more likely stabilized by the anionic POM ligand; (2) the μ_3-OH assignment is consistent with the elemental analysis results and charge balance (counterions: Rb^+ and K^+); (3) the experimental and computational torsional angles compare well (details given below); (4) the bond distances (Re1−O1: 2.162; Re2−O1: 2.186; Re3−O1: 2.156 Å) are similar to those in $[Re_3(CO)_9(\mu_3\text{-}OH)(\mu\text{-}OH)_3]^-$ (mean values: Re−O 2.167 Å), but longer than the ones in $[Re_3(CO)_9(\mu_3\text{-}O)(GlycH_{-3})]^{2-}$ (Glyc = glycerol; mean values: Re−O 2.122 Å);[10] (5) intramolecular hydrogen bonds are likely present between O1 and the bridging oxygen atoms in $[\alpha_2\text{-}P_2W_{17}O_{61}]^{10-}$ which can further stabilize the structure (Supporting Information, Figure S1).

Computational density functional theory (DFT) studies of two model systems, namely $[P_2W_{17}O_{61}\{Re(CO)_3\}_3(\mu_2\text{-}OH)(\mu_3\text{-}O)]^{10-}$ (**m1**) and $[P_2W_{17}O_{61}\{Re(CO)_3\}_3(\mu_2\text{-}OH)(\mu_3\text{-}OH)]^{9-}$ (**m2**), provide strong support for the structural assignment of **1**. In these model systems of **1**, the Rb^+ was replaced by a proton to capture the ion-pairing feature and to avoid the possible technical difficulties. The difference between **m1** and **m2** is the protonation state of the central μ_3-O1 unit in **1**. A comparison of the calculated important geometry parameters (such as the geometry of POMs, Re−O(POM) and Re-CO bond distances) of the model systems with their values in the experimentally reported complex **1** provides strong support for the structural assignment of **1**. As expected the calculated geometries of **m1** and **m2** are very close to each other and, in general, are in reasonable agreement with the values reported for **1**, except the Re(*n*)-O1 (*n* = 1−3) bond distances and improper torsion angle (Re2−Re1−Re3−O1; see Supporting Information, Figure S1). In **m2**, the calculated Re(*n*)-O1 (*n* = 1−3) bond distances are only 0.08−0.10 Å longer and the torsion angle is only 4.9° smaller than the experimental values for **1**. Although in **m1** the discrepancy of the calculated and experimental values of Re(*n*)-O1 (*n* = 1−3) bond distances is relatively small (calculated values are shorter by 0.02−0.04 Å), the improper torsion angle (Re2−Re1−Re3−O1) (of 3.4°) is almost 6.4 times smaller than its experimental value for **1**. These findings strongly support the assignment of a central μ_3-OH unit in **1**.

The charge-transfer studies in sensitized polyoxotitanate nanoclusters,[11] and in POM-supported monometal carbonyl complexes,[6] as well as in other POM−photosensitizer dyads,[12] inspired us to investigate the photochemical properties of **1**. As seen in Supporting Information, Figure S2a, the UV−vis absorption spectrum of **1** shows an intense broad absorption covering the entire UV and visible region extending to ∼700 nm with a high absorptivity ($\varepsilon_{400\ nm}$ ∼3,500 $M^{-1}\cdot cm^{-1}$ in water) comparable with many rhenium(I) polybipyridyl photosensitizers (e.g., $\varepsilon_{370\ nm}$ ∼2500 $M^{-1}\cdot cm^{-1}$ for $(bpy)Re(CO)_3Cl$ in MeCN).[13] The precursors $[\alpha_2\text{-}P_2W_{17}O_{61}]^{10-}$ and $[Re(CO)_3]^+$ only have the ligand-to-metal charge-transfer (LMCT) transitions below ∼350 nm, so this visible absorption of **1** is likely due to metal-to-polyoxometalate charge-transfer (MPCT) transition from the Re centers to the POM ligands.[6] The stability of **1** in water has also been evaluated by UV−vis absorption spectroscopy. A slow degradation process is observed over a period of two days (Supporting Information, Figure S2b and S2c).

The calculated frontier orbitals (Figure 2) and UV−vis absorption spectra (see Figure 3, Table 1 and Supporting Information, Table S6) of **m2** support the experimental conclusions given above and reveal important details. As seen in Figure 2, the HOMO orbital is entirely localized on the $[\{Re(CO)_3\}(\mu_2\text{-}OH)(\mu_3\text{-}OH)]$ fragment of $[P_2W_{17}O_{61}\{Re(CO)_3\}_3(\mu_2\text{-}OH)(\mu_3\text{-}OH)]^{9-}$, **m2**. Contributions from the Re1 and Re2 atoms to the HOMO are dominant. Close examination of this orbital reveals a noticeable overlap between the orbitals of Re2 and O3 (see Supporting Information, Figure S1 for atom notations). In contrast, the LUMO of **m2** is a

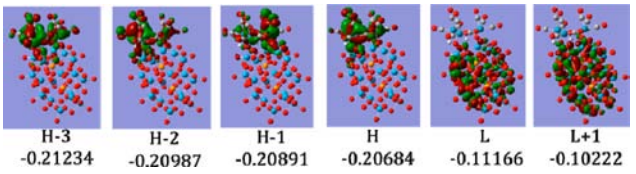

Figure 2. Several highest occupied (HOMO, or H) and lowest unoccupied (LUMO, or L) orbitals and their orbital energies (in Hartree) of the model complex **m2**.

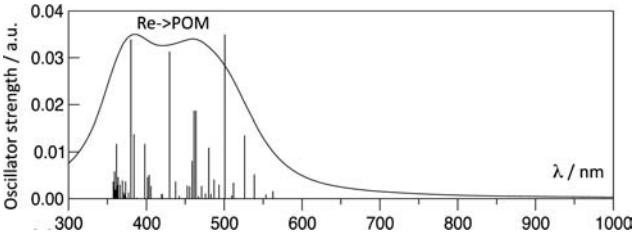

Figure 3. Simulation of UV−vis absorption spectrum of S_0 state of model complex **m2**.

dx.doi.org/10.1021/ic4018823 | *Inorg. Chem.* 2013, 52, 13490−13495

Table 1. Low Energy Singlet and Triplet Excited States of Complex m2

	E/eV	λ/nm	osc. str.	char.
T_1	2.152	576		H → L
S_1	2.203	562	0.0016	H → L
T_2	2.203	562		H−1 → L
S_2	2.239	553	0.0009	H−1 → L
T_3	2.263	547		H−3 → L
				H → L
S_3	2.301	538	0.0052	H−2 → L
T_4	2.287	542		H−2 → L
S_4	2.356	526	0.0135	H−3 → L

purely POM-based orbital consisting predominantly of W−O antibonding orbitals.

As in Figure 3, the simulated UV−vis absorption spectrum for the ground state (S_0) of complex **m2** has a relatively narrow double feature on the 350−550 nm range. All bright transitions that make up this feature are excitations from doubly occupied Re d orbitals to the virtual POM orbitals (Table 1). No excitations originating on a Re orbital and ending on a virtual Re orbital are found among the 50 calculated states (Supporting Information, Table S6). Such transitions can be expected to occur at wavelengths shorter than 350 nm.

The redox properties of **1** were studied by cyclic voltammetry (CV). As shown in Figure 4, scanning in the

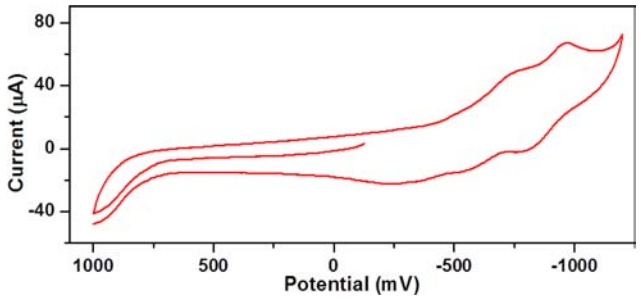

Figure 4. Cyclic voltammetry of 1.0 mM **1** in 20 mM sodium acetate buffer at pH 4.7 in the presence of 0.2 M $LiClO_4$. Potentials vs Ag/AgCl; Scan rate: 100 mV/s.

positive potential domain shows one irreversible peak at ∼0.9 V (vs Ag/AgCl) tentatively assigned to oxidation of Re(I) center(s) which results in film formation on the electrode surface. This film can be removed by scanning to the potential about −0.2 V. The cycling between −0.2 and 1.0 V produces the same CV curve. Several cycles between 0 and 1.0 V result in the complete disappearance of the peak at 0.9 V. In the negative potential domain, the CV is quasi-reversible with two poorly resolved cathodic peaks approximately at E_{pc} = −0.73, −0.96 V. In a reverse scan three peaks are observed at approximately E_{pa} = −0.77, −0.53, and −0.25 V. The first cathodic peak is likely to consist of two unresolved peaks. The width and low current of the CV peaks are consistent with slow electron transfer. To minimize the possible Frumkin effect, we increased the electrolyte concentration; however, no changes in the CV were observed (Supporting Information, Figure S7). The slow electron transfer rates are likely due to high reorganization energies in **1**. The negative-domain peaks are assigned to W(VI) to W(V) reductions. This is confirmed by spectroelectrochemistry (Figure 5a). Compound **1** shows good reversibility in spectroelectrochemical experiments, where the electro-

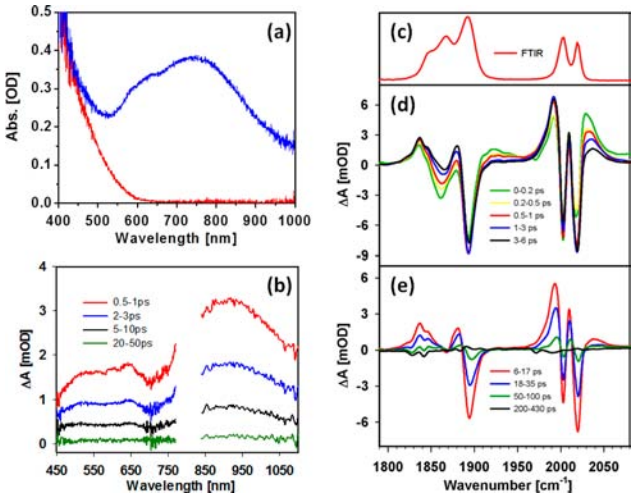

Figure 5. (a) Ground state UV−vis absorption spectra of **1** (red) and electrochemically reduced **1** (blue) generated at an applied potential of −0.65 V vs Ag/AgCl in sodium acetate buffer recorded in an electrochemical cell. (b) Average visible-to-near IR transient absorption spectra of **1** in CH_2Cl_2 at indicated delay time windows after 400 nm excitation. (c) Ground state FTIR spectrum of **1** in CH_2Cl_2. (d,e) Vis-pump/IR-probe transient spectra of **1** in CH_2Cl_2 at indicated delay times (d, 0−6 ps; e, 6−430 ps) windows after 400 nm excitation.

reduction and O_2-based reoxidation processes are repeated sequentially (more details below and in the Supporting Information).

Femtosecond visible pump−probe spectroscopy was used to study the charge-transfer dynamics. As shown in Figure 5b, the transient absorption spectra of **1** show a new broad absorption species with a maximum at ∼620 nm. Upon electrochemical reduction of **1** at multiple potentials, broad absorption bands (∼600−1000 nm) in different shapes appear with maxima around 600 to 700 nm (Figure 5a, Supporting Information, Figures S8 and S9), which are consistent with other compounds containing a reduced $[\alpha_2\text{-}P_2W_{17}O_{61}]^{10-}$ unit.[14] All these new absorption bands can be attributed to the well-documented W(V) d-d and W(V)−W(VI) intervalence charge-transfer (IVCT) transitions in the reduced Wells-Dawson POMs, known as "heteropoly blues".[15] Note that the electrochemical spectra also show some absorption in the near-IR region (∼800−1000 nm). We probed the transient spectra in this region and found an enhanced absorption feature, consistent with a "heteropoly blue" species,[16] containing a maximum at ∼920 nm (Figure 5b). The kinetics of this photoinduced absorption feature were monitored at 620 and 920 nm and fitted by a multiexponential function. The two traces show identical kinetics (Figure 5d, 5e, and Supporting Information, Figure S10). The best fit yields an instantaneous formation of the excited state within the time resolution of measurement (∼150 fs) and its biexponential decay (∼0.4 and 4.8 ps) to form a "hot" ground state) (Supporting Information, Table S2; see more details below).

Time-resolved infrared spectroscopy provides detailed information on the excited states of rhenium carbonyl complexes owing to their high sensitivity to electron-density distribution. Since the entire molecule has low symmetry (C_1), the three Re(I) centers are asymmetrically bridged, and each $[Re(CO)_3]^+$ moiety has local C_{3v} symmetry, the triple sets of three IR-active C−O stretching modes, two symmetric and one

dx.doi.org/10.1021/ic4018823 | Inorg. Chem. 2013, 52, 13490−13495

antisymmetric, are coupled and overlapped. As shown in Figure 5c, the ground-state FTIR spectra are complicated and show approximately 3:2 stretching bands in the lower and higher wavelength regions respectively (1847, 1868, 1892 cm^{-1}; 2002, 2019 cm^{-1}).

Figure 5d/5e shows the transient absorption spectra in the short and long time scales. Excitation into the MPCT band at 400 nm results in the depletion of the ν(CO) ground state bands at approximately 1865, 1894, 2003, and 2020 cm^{-1} and instantaneous formation of two new blue-shifted absorption bands at ~1924 and 2031 cm^{-1}, relative to the ground-state positions, consistent with the formation of the MPCT excited state. The dynamic of the excited state absorption bands at 1924 and 2031 cm^{-1} can be fit to a triexponential function with $\tau_1 = 60 \pm 20$ fs (formation time), $\tau_2 = 0.50 \pm 0.4$ ps and $\tau_3 = 5 \pm 2$ ps and $\tau_1 = 60 \pm 20$ fs (formation time), $\tau_2 = 0.87 \pm 0.3$ ps and $\tau_3 = 4.7 \pm 2$ ps, respectively. The decay components (τ_2, τ_3), which agree well with the decay kinetics at 920 and 620 nm (Figure 5b and 6a), can be assigned to the decay of MPCT

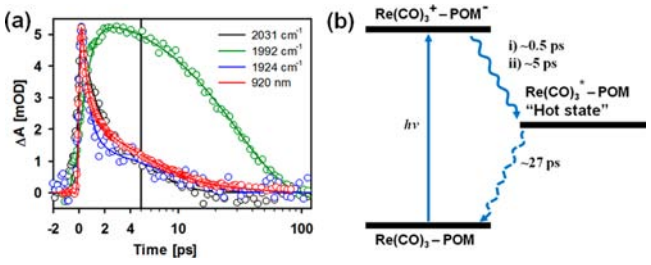

Figure 6. (a) Transient kinetics of **1** in CH_2Cl_2 at 920 nm (red), 1924 cm^{-1} (blue), 1992 cm^{-1} (green), and 2031 cm^{-1} (black) after 400 nm excitation. Solid lines show the multiple-exponential fits. The delay time is on a linear scale in the left panel (−2 to 5 ps) and a logarithmic scale in the right panel (5−120 ps). (b) Energy-level diagram of the electron-transfer steps involved in the charge-separation processes in **1**.

excited state. The reason for the biexponential decay kinetics is not clear, although it may indicate an energy relaxation process within the excited state. The excited state decay leads to the formation of two new positive absorption bands at 1837 and 1992 cm^{-1}, that are red-shifted relative to the parent bands (Figure 6a, Supporting Information, Figure S11 and Table S3) and can be assigned to the vibrationally excited molecules in the ground electronic state. Once the formation of "hot" ground state molecules (HGA) is completed within ~10 ps (Figure 5d/5e), the TA spectra show the concomitant recovery of the ground state bleach (GSB) and decay of the HGA, which can be attributed to the vibrational cooling process. Fitting of the GSB recovery and HGA decay kinetics yields a cooling time constant of approximately 27 ps (Figure 6a and Supporting Information, Table S3).

To completely understand the vibrational dynamics of ν(CO) in **1** and the nature of the hot ground state, we performed transient IR-pump/IR-probe experiments monitoring the vibrational relaxation following IR excitation at ~1870 cm^{-1} and 2007 cm^{-1}, respectively. As shown in the Supporting Information, Figure S12, at early delay times the transient IR-pump/IR-probe spectra consist of instantaneous bleaches of the ground state CO stretches ($\upsilon = 0$ to $\upsilon = 1$ transition) and the corresponding excited state absorptions ($\upsilon = 1$ to $\upsilon = 2$ transition) at ~1884, 1876, 1996, and 2013 cm^{-1}. Spectra at longer delay times show that all the GSB and HGA bands recover and decay on very similar time scales. These results are consistent with the relaxation of the molecules back to the ground vibrational state. The results and fitting parameters are given in Supporting Information, Figure S13 and Table S4. Both the GSB and HGA are characterized by ultrafast response times in the subpicosecond time scale following by a biexponential decay of the $\upsilon = 1$ population with time constants of approximately $\tau_2 = 0.3$ ps and $\tau_3 = 26$ ps. All traces show nearly identical kinetics with values within the experimental error, implying that their relaxation pathways are the same. We attribute the ultrafast decay component to the coupling between the different carbonyl stretching modes, and the slower decay component to the total vibrational population relaxation time. Our results are in agreement with previous studies on the vibrational relaxation dynamics of several metal carbonyl complexes.[17] Both the spectra and kinetics of the hot ground state generated by IR excitation of the CO stretching modes (Supporting Information, Figure S12 and S13) agree well with the hot ground state generated by 400 nm excitation of the MPCT state (Figure 5e), suggesting that HGA features in the latter are due to the formation of $\upsilon = 1$ states of the CO stretching modes upon relaxation from the excited state. Finally, a general energy-level diagram displaying the MPCT process in this novel inorganic donor (trirhenium)−acceptor (POM) system is shown in Figure 6b.

To further complement the details of reported IR and transient absorption spectra of compound **1**, we again turned to computation. Inspection of the S_0 IR spectrum shows that the CO portions of the spectrum appear in two manifolds, a broad, structured triplet in the 1850−1960 cm^{-1} range and a narrower doublet in the 2020−2080 cm^{-1} range (Figure 7 and Table 2),

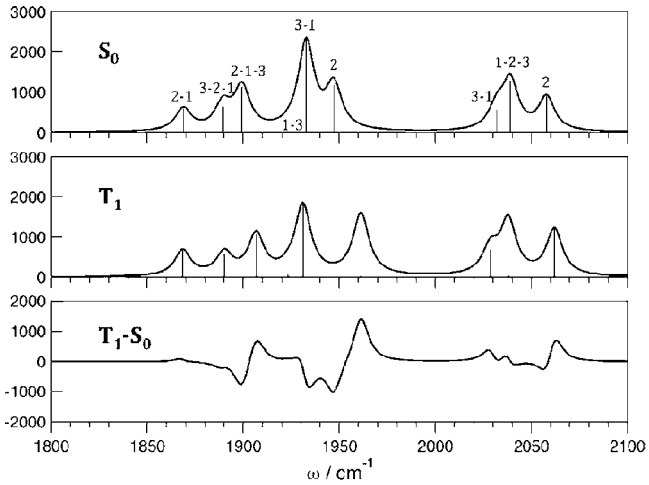

Figure 7. IR spectra of the model complex **m2** in the CO range of S_0 (top), T_1 (middle), and difference spectra (bottom). Peak labels show Re−Re−Re center involvement in the order of decreasing magnitude, where the index for each Re can be 1, 2 or 3.

which is consistent with the experiments. Individual features of each manifold are assigned based on the Re center involvement, that is, the first peak involves Re1 and Re2 centers, with very little Re3, and the second peak is mainly Re3 with smaller mixture of Re1 and Re2. The assignments reveal that the triplet manifold consists of six distinct out-of-phase superpositions of antisymmetric local CO stretches. In all six peaks, up to five CO bond stretches are strongly involved. The doublet manifold is composed of three peaks, which are out-of-phase (the first two)

dx.doi.org/10.1021/ic4018823 | Inorg. Chem. 2013, 52, 13490−13495

Table 2. Vibrational Frequencies (ω; cm^{-1}) and IR Intensities (km/mol) of the Carbonyl Groups of m2[a]

$\omega(S_0)$	IR(S_0)	$\omega(T_1)$	IR(T_1)	character
1868	601	1868	680	Re2 + Re1
1889	671	1890	590	Re3 + Re2 + Re1
1899	1140	1906	1076	Re2 + Re1 + Re3
1925	35	1923	78	Re1 + Re3
1932	2361	1931	1861	Re3 + Re1
1947	1185	1961	1657	Re2
2031	580	2028	687	Re3 + Re1
2039	1302	2037	1443	Re1 + Re2 + Re3
2057	906	2062	1239	Re2

[a]The combinations of Re centers are in the order of decreasing magnitude according to contribution.

and in-phase (the third) superpositions of symmetric local CO stretches.

The T_1 state of **m2** is characterized by the HOMO−LUMO excitation, which removes an electron mainly from Re1 and Re2 centers and to a lesser degree from the Re3 center. Electronic spin density shows that there is ∼0.8 of unpaired spin on the Re2−O3 bond. The IR CO spectrum reflects the change experienced by the electron density. The deviations of the T_1 line shape from that of S_0 occur at frequencies with the most activity from the Re2 group of CO's. At 1900 cm^{-1}, the 2−1−3 peak shifts to the blue by about 10 cm^{-1}. There is an even larger blue shift at ∼1950 cm^{-1} where there is strong CO activity on the Re2 center. Another shift can be seen at ∼2060 cm^{-1} where another dominant CO mode on Re2 is located. Although the agreement of the computed and measured IR spectra is not quantitative, the observed blue shift of the CO stretching bands upon excitation of the complex is well reproduced in the computed spectrum, consistent with the nature of an MPCT transition.

CONCLUSIONS

In conclusion, we report for the first time a molecular representation of the much studied TiO_2−$Ru(bpy)_3$ Grätzel diad systems in the form of an inorganic dye donor covalently bonded to a redox active metal oxide-like POM acceptor, $[P_2W_{17}O_{61}\{Re(CO)_3\}_3\{ORb(H_2O)\}(\mu_3\text{-}OH)]^{9-}$, **1**. Comprehensive investigation of the photophysical properties of **1** using computational and two different time-resolved spectroscopic methods clearly reveal the presence of a metal-to-polyoxometalate charge transfer (MPCT). The stepwise mechanism of charge-separation and charge-recombination process has been established.

However, since the system does not emit, the excited state energy and potentials are not experimentally accessible. The lifetime of this charge-separated excited state is short, and thus capturing it to drive a chemical reaction is challenging. Ongoing work attempts to capture these short-lived but visible-light-accessible CT states by pairing electron accepting cations with the polyanion, **1**.

ASSOCIATED CONTENT

Supporting Information

X-ray crystallographic data for $Rb_{8.1}K_{0.9}$-**1**·$45H_2O$ in CIF format. Synthesis and characterization, crystallographic data, spectroelectrochemistry studies, transient spectral and kinetic analysis, details of computational procedures and modeling. This material is available free of charge via the Internet at http://pubs.acs.org.

AUTHOR INFORMATION

Corresponding Authors

*E-mail: tlian@emory.edu (T.L.).
*E-mail: dmusaev@emory.edu (D.G.M.).
*E-mail: chill@emory.edu (C.L.H.).

Present Address

[†]Escuela de Física, Universidad Nacional de Colombia Sede Medellín, A.A. 3840, Medellín, Colombia.

Notes

The authors declare no competing financial interest.

ACKNOWLEDGMENTS

This work was funded by the U.S. Department of Energy, Office of Basic Energy Sciences, Solar Photochemistry Program (DE-FG02-07ER-15906) to C.L.H., T.L., and D.G.M. The authors also gratefully acknowledge NSF MRI-R2 instrument grant (CHE-0958205) and use of the resources of the Cherry Emerson Center for Scientific Computation. We thank Dr. John Bacsa and Jordan Sumliner for assistance on X-ray diffraction and spectroelectrochemistry experiments, respectively.

REFERENCES

(1) (a) Serpone, N.; Pelizzetti, E.; Gratzel, M. *Coord. Chem. Rev.* **1985**, *64*, 225. (b) Grätzel, M. *Nature* **2001**, *414*, 338. (c) Ardo, S.; Meyer, G. J. *Chem. Soc. Rev.* **2009**, *38*, 115.

(2) (a) Youngblood, W. J.; Lee, S.-H. A.; Kobayashi, Y.; Hernandez-Pagan, E. A.; Hoertz, P. G.; Moore, T. A.; Moore, A. L.; Gust, D.; Mallouk, T. E. *J. Am. Chem. Soc.* **2009**, *131*, 926. (b) Brimblecombe, R.; Koo, A.; Dismukes, G. C.; Swiegers, G. F.; Spiccia, L. *J. Am. Chem. Soc.* **2010**, *132*, 2892. (c) Li, L.; Duan, L.; Xu, Y.; Gorlov, M.; Hagfeldt, A.; Sun, L. *Chem. Commun.* **2010**, *46*, 7307. (d) Moore, G. F.; Blakemore, J. D.; Milot, R. L.; Hull, J. F.; Song, H.-e.; Cai, L.; Schmuttenmaer, C. A.; Crabtree, R. H.; Brudvig, G. W. *Energy Environ. Sci.* **2011**, *4*, 2389. (e) Song, W.; Brennaman, M. K.; Concepcion, J. J.; Jurss, J. W.; Hoertz, P. G.; Luo, H.; Chen, C.; Hanson, K.; Meyer, T. J. *J. Phys. Chem. C* **2011**, *115*, 7081. (f) Li, G.; Sproviero, E. M.; McNamara, W. R.; C. S., R., III; Crabtree, R. H.; Brudvig, G. W.; Batista, V. S. *J. Phys. Chem. B* **2010**, *114*, 14214.

(3) (a) Lin, W.; Frei, H. *J. Am. Chem. Soc.* **2005**, *127*, 1610. (b) Han, H.; Frei, H. *J. Phys. Chem. C* **2008**, *112*, 16156. (c) Nakamura, R.; Okamoto, A.; Osawa, H.; Irie, H.; Hashimoto, K. *J. Am. Chem. Soc.* **2007**, *129*, 9596. (d) Takashima, T.; Yamaguchi, A.; Hashimoto, K.; Nakamura, R. *Chem. Commun.* **2012**, *48*, 2964.

(4) (a) Nozik, A. J. *Annu. Rev. Phys. Chem.* **1978**, *29*, 189. (b) Tan, M. X.; Laibinis, P. E.; Nguyen, S. T.; Kesselman, J. M.; Stanton, C. E.; Lewis, N. S. In *Progress in Inorganic Chemistry*; Karlin, K. D., Ed.; Wiley & Sons: New York, 1994; Vol. *41*, p 21; (c) Prezhdo, O. V. *Acc. Chem. Res.* **2009**, *42*, 2005. (d) Hoffmann, M. R.; Martin, S. T.; Choi, W.; Bahnemann, D. W. *Chem. Rev.* **1995**, *95*, 69. (e) Nozik, A. J.; Beard, M. C.; Luther, J. M.; Law, M.; Ellingson, R. J.; Johnson, J. C. *Chem. Rev.* **2010**, *110*, 6873.

(5) (a) Pope, M. T.; Müller, A. *Angew. Chem., Int. Ed.* **1991**, *30*, 34. (b) Special Thematic Issue on Polyoxometalates; Hill, C. L., Ed.; *Chem. Rev.***1998**; Vol. *98*, No. 1; (c) Hill, C. L.; Prosser-McCartha, C. M. *Coord. Chem. Rev.* **1995**, *143*, 407. (d) Okuhara, T.; Mizuno, N.; Misono, M. *Adv. Catal.* **1996**, *41*, 113. (e) Neumann, R. *Prog. Inorg. Chem.* **1998**, *47*, 317. (f) Long, D.-L.; Tsunashima, R.; Cronin, L. *Angew. Chem., Int. Ed.* **2010**, *49*, 1736. (g) Miras, H. N.; Yan, J.; Long, D.-L.; Cronin, L. *Chem. Soc. Rev.* **2012**, *41*, 7403.

(6) Zhao, C.; Huang, Z.; Rodríguez-Córdoba, W.; Kambara, C. S.; O'Halloran, K. P.; Hardcastle, K. I.; Musaev, D. G.; Lian, T.; Hill, C. L. *J. Am. Chem. Soc.* **2011**, *133*, 20134.

(7) (a) Quiñonero, D.; Wang, Y.; Morokuma, K.; Khavrutskii, L. A.; Botar, B.; Geletii, Y. V.; Hill, C. L.; Musaev, D. G. *J. Phys. Chem.* **2006**, *110*, 170. (b) Wang, Y.; Zheng, G.; Morokuma, K.; Geletii, Y. V.; Hill, C. L.; Musaev, D. G. *J. Phys. Chem. B* **2006**, *110*, 5230.
(8) (a) Kulkarni, A.; Lobo-Lapidus, R. J.; Gates, B. C. *Chem. Commun.* **2010**, *46*, 5997. (b) Hu, A. G.; Neyman, K. M.; Staufer, M.; Belling, T.; Gates, B. C.; Rosch, N. *J. Am. Chem. Soc.* **1999**, *121*, 4522. (c) Fierro-Gonzalez, J. C.; Kuba, S.; Hao, Y. L.; Gates, B. C. *J. Phys. Chem. B* **2006**, *110*, 13326.
(9) (a) Knoth, W. H. *J. Am. Chem. Soc.* **1979**, *101*, 2211. (b) Besecker, C. J.; Klemperer, W. G. *J. Am. Chem. Soc.* **1980**, *25*, 7598. (c) Klemperer, W. G.; Main, D. J. *Inorg. Chem.* **1990**, *29*, 2355. (d) Siedle, A. R.; Lyon, P. A.; Hodgson, K. O.; Roe, A. L. *Inorg. Chem.* **1987**, *26*, 219. (e) Nagata, T.; Pohl, B. M.; Weiner, H.; Finke, R. G. *Inorg. Chem.* **1997**, *36*, 1366. (f) Besserguenev, A. V.; Dickman, M. H.; Pope, M. T. *Inorg. Chem.* **2001**, *40*, 2582. (g) Villanneau, R.; Delmont, R.; Proust, A.; Gouzerh, P. *Chem.—Eur. J.* **2000**, *6*, 1184. (h) Villanneau, R.; Proust, A.; Robert, F.; Gouzerh, P. *Chem.—Eur. J.* **2003**, *9*, 1982. (i) Sadakane, M.; Iimuro, Y.; Tsukuma, D.; Bassil, B. S.; Dickman, M. H.; Kortz, U.; Zhang, Y.; Ye, S.; Ueda, W. *Dalton Trans.* **2008**, 6692. (j) Niu, J.; Yang, L.; Zhao, J.; Ma, P.; Wang, J. *Dalton Trans.* **2011**, *40*, 8298. (k) Zhao, J.; Zhao, J.; Ma, P.; Wang, J.; Niu, J.; Wang, J. *J. Mol. Struct.* **2012**, *1019*, 61. (l) Zhao, C.; Kambara, C. S.; Yang, Y.; Kaledin, A. L.; Musaev, D. G.; Lian, T.; Hill, C. L. *Inorg. Chem.* **2013**, *52*, 671.
(10) (a) Alberto, R.; Egli, A.; Abram, U.; Hegetschweiler, K.; Gramlich, V.; Schubiger, P. A. *J. Chem. Soc., Dalton Trans.* **1994**, 2815. (b) Egli, A.; Hegetschweiler, K.; Alberto, R.; Abram, U.; Schibli, R.; Hedinger, R.; Gramlich, V.; Kissner, R.; Schubiger, P. A. *Organometallics* **1997**, *16*, 1833. (c) Herrmann, W. A.; Egli, A.; Herdtweck, E.; Alberto, R.; Baumgärtner, F. *Angew. Chem., Int. Ed.* **1996**, *35*, 432. (d) Hinrichs, M.; Hofbauer, F. R.; Klufers, P. *Chem.—Eur. J.* **2006**, *12*, 4675.
(11) (a) Benedict, J. B.; Freindorf, R.; Trzop, E.; Cogswell, J.; Coppens, P. *J. Am. Chem. Soc.* **2010**, *132*, 13669. (b) Snoeberger, R. C.; Young, K. J.; Tang, J.; Allen, L. J.; Crabtree, R. H.; Brudvig, G. W.; Coppens, P.; Batista, V. S.; Benedict, J. B. *J. Am. Chem. Soc.* **2012**, *134*, 8911. (c) Sokolow, J. D.; Trzop, E.; Chen, Y.; Tang, J.; Allen, L. J.; Crabtree, R. H.; Benedict, J. B.; Coppens, P. *J. Am. Chem. Soc.* **2012**, *134*, 11695.
(12) (a) Matt, B.; Xiang, X.; Kaledin, A. L.; Han, N.; Moussa, J.; Amouri, H.; Alves, S.; Hill, C. L.; Lian, T.; Musaev, D. G.; Izzet, G.; Proust, A. *Chem. Sci.* **2013**, *4*, 1737. (b) Odobel, F.; Séverac, M.; Pellegrin, Y.; Blart, E.; Fosse, C.; Cannizzo, C.; Mayer, C. R.; Elliott, K. J.; Harriman, A. *Chem.—Eur. J.* **2009**, *15*, 3130. (c) Harriman, A.; Elliott, K. J.; Alamiry, M. A. H.; Pleux, L. L.; Séverac, M.; Pellegrin, Y.; Blart, E.; Fosse, C.; Cannizzo, C.; Mayer, C. R.; Odobel, F. *J. Phys. Chem. C* **2009**, *113*, 5834. (d) Allain, C.; Favette, S.; Chamoreau, L.-M.; Vaissermann, J.; Ruhlmann, L.; Hasenknopf, B. *Eur. J. Inorg. Chem.* **2008**, 3433.
(13) Ziessel, R.; Juris, A.; Venturi, M. *Inorg. Chem.* **1998**, *37*, 5061.
(14) (a) Haraguchi, N.; Okaue, Y.; Isobe, T.; Matsuda, Y. *Inorg. Chem.* **1994**, *33*, 1015. (b) Sun, W.; Yang, F.; Liu, H.; Kong, J.; Jin, S.; Xie, G.; Deng, J. *J. Electroanal. Chem.* **1998**, *451*, 49. (c) Gao, G.; Xu, L.; Wang, W.; An, W.; Qiu, Y. *J. Mater. Chem.* **2004**, *14*, 2024.
(15) (a) Sanchez, C.; Livage, J.; Launay, J. P.; Fournier, M.; Jeannin, Y. *J. Am. Chem. Soc.* **1982**, *104*, 3194. (b) Kozik, M.; Hammer, C. F.; Baker, L. C. W. *J. Am. Chem. Soc.* **1986**, *108*, 7627. (c) Kozik, M.; Casañ-Pastor, N.; Hammer, C. F.; Baker, L. C. W. *J. Am. Chem. Soc.* **1988**, *110*, 7697. (d) Papaconstantinou, E. *Chem. Soc. Rev.* **1989**, *18*, 1. (e) Yamase, T. *Chem. Rev.* **1998**, *98*, 307. (f) Renneke, R. F.; Kadkhodayan, M.; Pasquali, M.; Hill, C. L. *J. Am. Chem. Soc.* **1991**, *113*, 8357. (g) Hill, C. L.; Kozik, M.; Winkler, J.; Hou, Y.; Prosser-McCartha, C. M. *Adv. Chem. Ser.* **1993**, *238*, 243.
(16) (a) Yamase, T.; Usami, T. *J. Chem. Soc., Dalton Trans.* **1988**, 183. (b) Duncan, D. C.; Netzel, L., T.; Hill, C. L. *Inorg. Chem.* **1995**, *34*, 4640.
(17) (a) Beckerle, J. D.; Casassa, M. P.; Cavanagh, R. R.; Heilweil, E. J.; Stephenson, J. C. *Chem. Phys.* **1992**, *160*, 487. (b) Tokmakoff, A.; Sauter, B.; Kwok, A. S.; Fayer, M. D. *Chem. Phys. Lett.* **1994**, *221*, 412. (c) Lian, T.; Bromberg, S. E.; Yang, H.; Proulx, G.; Bergman, R. G.; Harris, C. B. *J. Am. Chem. Soc.* **1996**, *118*, 3769. (d) Gabrielsson, A.; Hartl, F.; Zhang, H.; Smith, J. R. L.; Towrie, M.; Antonín Vlček, J.; Perutz, R. N. *J. Am. Chem. Soc.* **2006**, *128*, 4253.